The 19th International Topical Meeting on Nuclear Reactor Thermal Hydraulics (NURETH-19) Log nr.: 36362
Brussels, Belgium, March 6 - 11, 2022

EXPERIMENTS FOR THE MECHANISMS DETERMINING CHF AND HTC VALUES IN NANOFLUID POOL BOILING

Ren Ning, Koki Nakano, Yutaro Umehara, Yasuo Koizumi, and Tomio Okawa
The University of Electro-Communications
1-5-1, Chofugaoka, Chofu-shi, Tokyo 182-8585, Japan
ning.ren@eel.mi.uec.ac.jp; nakano.koki@eel.mi.uec.ac.jp; umehara@eel.mi.uec.ac.jp,
koizumiy@shinshu-u.ac.jp; okawa.tomio@uec.ac.jp

ABSTRACT

It has been reported that in nanofluid pool boiling, the critical heat flux (CHF) is usually enhanced but the boiling heat transfer coefficient (HTC) is augmented in some experiments and deteriorated in others. Clear reasons to cause these results have not been elucidated yet. In this work, pool boiling experiments were performed using water-based nanofluids. TiO_2, Al_2O_3 and SiO_2 were used as the nanoparticle materials and all the experiments were conducted at the atmospheric pressure. As reported by previous investigators, the CHF was enhanced in all the cases, but the HTC was not changed for TiO_2, augmented for Al_2O_3 and deteriorated for SiO_2. To understand these results, the thickness, the surface roughness, the wickability, and the total mass of the nanoparticle layer formed on the heat transfer surface during nucleate boiling were measured. Generally, the thickness, the total mass and the surface roughness increased with an increase in the heat flux. The wickability also increased with an increase in the heat flux since the capability to suck liquid improves if the nanoparticle layer thickness increases. Ability of the nanoparticle layer to such the liquid was conjectured to be the main cause of the CHF enhancement in nanofluid pool boiling. The nanoparticle layer may act as the thermal insulation material and the nanoparticles suspended in liquid improves the thermal conductivity. Thus, the nanoparticles in the layer deteriorates the HTC and those in liquid improves it. It was considered that the HTC of nanofluid pool boiling was determined depending on the competition between the deterioration caused by the thermal-insulation effect of the nanoparticle layer and the improvement caused by the bulk fluid effect of the liquid thermal conductivity.

KEYWORDS
Nanofluid; Pool boiling; CHF; Heat transfer coefficient; Mechanism

1. INTRODUCTION

In comparison with ordinary heat transfer mechanisms such as heat conduction and single-phase forced-convective heat transfer, extremely high heat transfer coefficient is achieved in nucleate boiling [1]. Thus, it is regarded as a particularly important heat transfer mechanism and utilized in a variety of industrial applications including iron-manufacturing process, evaporation tube in boilers, reactor core in BWRs, steam generator in PWRs and FBRs, cooling of high-power-density electronic devices, and so on. In pursuing further enhancement of boiling heat transfer, two factors are of fundamental importance [2-4]. One is the heat transfer coefficient (HTC) and the other is the critical heat flux (CHF). If HTC is improved, heat transfer rate can be enhanced under the condition of the same temperature difference while temperature difference can be reduced under the condition of the same heat flux. Nucleate boiling is a high-performance heat transfer mechanism as described above. If the heat flux exceeds a certain value called CHF, however, the heat transfer surface is covered completely with vapor. Since the vapor acts as a thermal insulation material, this causes a drastic degradation of the heat transfer rate under the same temperature difference

condition while a rapid increase in the heat transfer surface temperature under the same heat flux condition. Thus, CHF determines the practical upper limit of the heat transfer rate in many industrial applications.

The use of nanofluid that is the colloidal dispersion of nano-meter sized solid particles in base liquid is spotlighted as a working liquid to enhance the heat transfer performance of nucleate boiling [5-7]. Many nucleate pool boiling experiments have been conducted so far to show that adding nanoparticles causes deterioration or enhancement of HTC depending on experimental conditions while it consistently improves CHF [8, 9]. The mechanisms to cause these heat transfer performance modifications have also been studied extensively. Addition of nanoparticles into the base liquid causes noticeable change in the thermal-hydraulic properties such as an increase in thermal conductivity and an increase or a decrease in surface tension [7, 8, 10]. Separately, nanoparticles are deposited to the heat transfer surface during nucleate boiling in nanofluid to alter the surface properties such as roughness, wettability and wickability [11, 12]. Thus, the modification of the heat transfer characteristics in nanofluid can be attributed to the bulk effect associated with the nanoparticles in liquid [13] and/or the surface effect associated with the nanoparticles deposited on the heat transfer surface [9]. As for CHF for structured hydrophilic surfaces, Rahman et al. [14] showed that the data of CHF enhancement ratio accumulated under various experimental conditions tend to increase linearly with an increase in the wickability that is one of the main factors representing the surface properties. It is therefore expected that the CHF enhancement in nanofluid is also largely dependent on the wickability.

In the case of nanofluid nucleate boiling, difficulty in specifying the mechanisms to cause heat transfer characteristics variations arises from the fact that the modifications of liquid properties and surface properties occur simultaneously. In addition, Okawa et al. [15] reported that nanoparticle deposition and consequently heat transfer surface properties continue to vary during nucleate boiling. Zuhairi Sulaiman et al. [16] and Watanabe et al. [17] further showed that detachment as well as deposition of nanoparticles occur during nucleate boiling since the adhesion of nanoparticles on the heat transfer surface is not always strong.

The literature survey presented above shows that experimental information on the variations of the heat transfer surface characteristics during nucleate boiling is indispensable to understand the mechanisms to cause variations of HTC and CHF in nucleate boiling in nanofluids. Thus, in the present work, increasing the heat flux gradually in the nucleate boiling in nanofluid, dependences of HTC and CHF on several heat transfer surface properties are explored experimentally. Based on the experimental data accumulated in this work, discussion is made on the mechanisms of the variations of HTC and CHF in nanofluid nucleate boiling.

2. DESCRIPTIONS OF EXPERIMENT

2.1. Experimental Apparatus

The experimental apparatus used in this work is shown in Fig. 1. The experimental vessel was 144 mm in inner diameter and 170 mm in height and its main body was made of transparent polycarbonate. The vessel contained an immersion heater, a dimroth condenser, and a calibrated type-K thermocouple accurate within ±0.3K. The circular end face of a copper block containing nine cartridge heaters were used as the heat transfer surface. The top surface was 20 mm in diameter and set at the bottom of the boiling vessel horizontally. Each cartridge heater was 7.3 mm in diameter and 45 mm in length and its power was 100 W. The maximum achievable heat flux was hence calculated 2.86 MW/m^2. The total power of the cartridge heaters was controlled using a volt slider. Five calibrated type-K thermocouples accurate within ±0.3K were positioned in the centerline of the copper block to calculate the heat flux q and the wall superheat ΔT using the Fourier law. The distances of the thermocouples from the top surface were 3, 8, 13, 18, 33, respectively. The heat transfer surface was flush with the stainless-steel plate of 2 mm in thickness. The copper block and the stainless-steel plate were connected smoothly using the electron-beam welding technique so as to

avoid anomalous boiling at the connection. During the experiment, the side walls of the boiling vessel and copper block were covered with thermal insulation material to reduce heat loss.

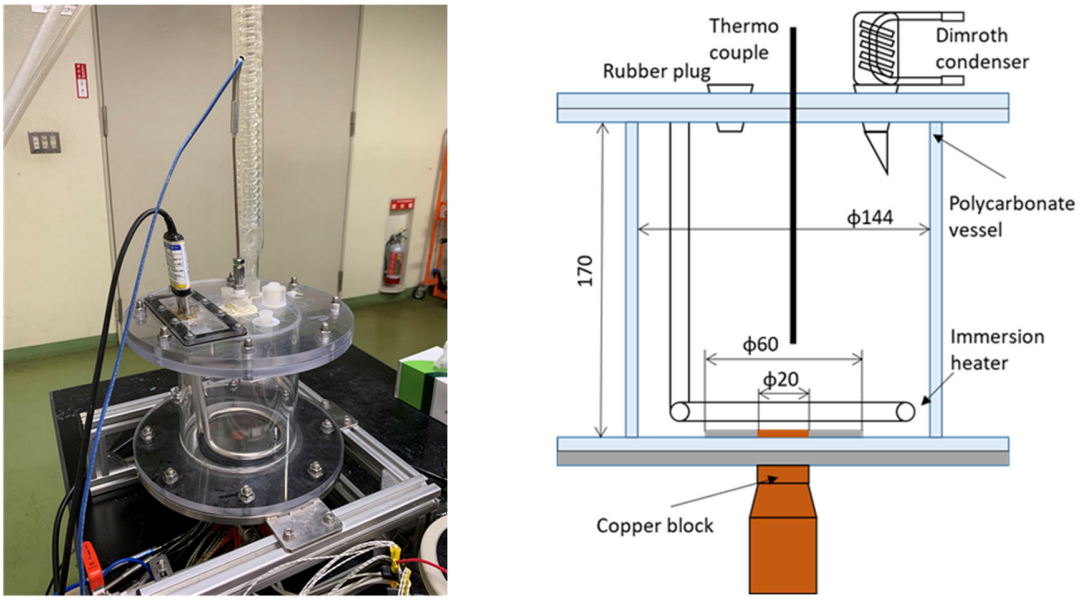

(a) Photo (b) Schematic diagram

Figure 1. Photo and Schematic diagram of experimental apparatus.

2.2. Preparation of Nanofluid

As the material of nanoparticles, TiO_2 (Aeroxide TiO_2 P25; mixture of 80% anatase and 20% rutile), Al_2O_3 (Aeroxide Alu C), and SiO_2 (Aeroxide 90 G) were used. These nanoparticles were manufactured by Evonik Industries. To prepare the nanofluid, 750mg, 75mg of nanoparticles were weighed using an electronic balance accurate to within ±0.07 mg (HR-202i, A&D Co., Ltd.). The weighed nanoparticles were then mixed with 200 ml of distilled water and ultrasonic excitation at 430 kHz was performed for 3 hours using an ultrasonic bath (QR-003, Kaijo Co., Ltd.). These procedures were considered sufficient to ensure stable particle dispersion since no noticeable particle sedimentation was found even 24 hours after the nanofluid preparation.

2.3. Preparation of Heat Transfer Surface

Prior to each experimental run, the heat transfer surface was polished using sandpaper of #600, #1000 and cleaned using an ultrasonic bath for 1 hour to eliminate nanoparticles on the original surface. Then, it was polished using metal polishing paste and cleaned using acetone to make the surface in fairly the same condition. To test if the initial surface is in the same condition, the surface wettability was measured using a contact angle goniometer (PG-X, Fibro System AB) to confirm that the contact angle was within the prescribed range of 90±5°.

2.4. Experimental Procedure

After setting the heating device at the bottom of the experimental vessel, 1300 ml of distilled water was supplied and saturated pool boiling condition was maintained in the vessel using the immersion heater for 1 hour for degassing. Then, the rubber plug on the top of the vessel was removed to supply nanofluid. The amounts of distilled water and nanofluid were adjusted so as to get the nanoparticle concentration in the working liquid at desired value. The rubber plug was placed on the original position after this procedure.

Then, the power of the immersion heater and the water flow rate to the condenser were controlled so as to maintain the test liquid at the saturation temperature.

After the above-described preparations, electric power was applied to the cartridge heaters embedded in the copper block step by step. The temperature data measured by the thermocouples were recorded every 1s throughout the experiment. After each stepwise increase of the heater power, temperature in the copper block increased asymptotically. Thus, the heater power was increased to the next level after the steady state was reached. The main experimental parameters were the nanoparticle material (TiO_2, Al_2O_3 and SiO_2) and the nanoparticle concentration (0.05 and 0.5 g/L). Experiments were conducted four times for the same condition to obtain the experimental information on the surface properties at different heat flux levels. In the first run, the heater power was increased till the copper block temperature started to keep increasing and the heat flux value at this occasion was regarded as CHF. In the second, third and fourth runs, the heat flux was increased step by step till it reached 25, 50 and 80% of CHF, respectively. During the experiment, the layer of nanoparticles was formed on the heat transfer surface. After each experimental run, the surface wickability was measured using the method developed by Rahman et al. [14]. Namely, a capillary glass tube of 0.5 mm in diameter was filled with distilled water and the hanging liquid surface from the lower end of the tube was let touch the heat transfer surface. Then, the water was sucked by the nanoparticle layer on the surface. The descending speed of the water level in the tube was measured using a high-speed camera to calculate the volume flow rate V_0. The wickability Wi is calculated by

$$Wi = \frac{V_0 \rho_l}{\rho_v^{1/2}[\sigma g(\rho_l - \rho_v)]^{1/4}} \tag{1}$$

where σ is the surface tension, g is the gravitational acceleration, and ρ_l and ρ_v are the liquid and vapor densities, respectively. Since the droplet which was placed on the nanoparticle coated surface was sucked into the nanoparticle layer, the contact angle was indeterminate in the present experiment. After the measurement of V_0, the mean roughness Ra and thickness δ of the nanoparticle layer was measured using a laser-microscope. Typical microscope images are depicted in Fig. 2. Finally, all the nanoparticles deposited on the heat transfer surface was scraped off to measure the total mass of the nanoparticle layer M using the electronic balance.

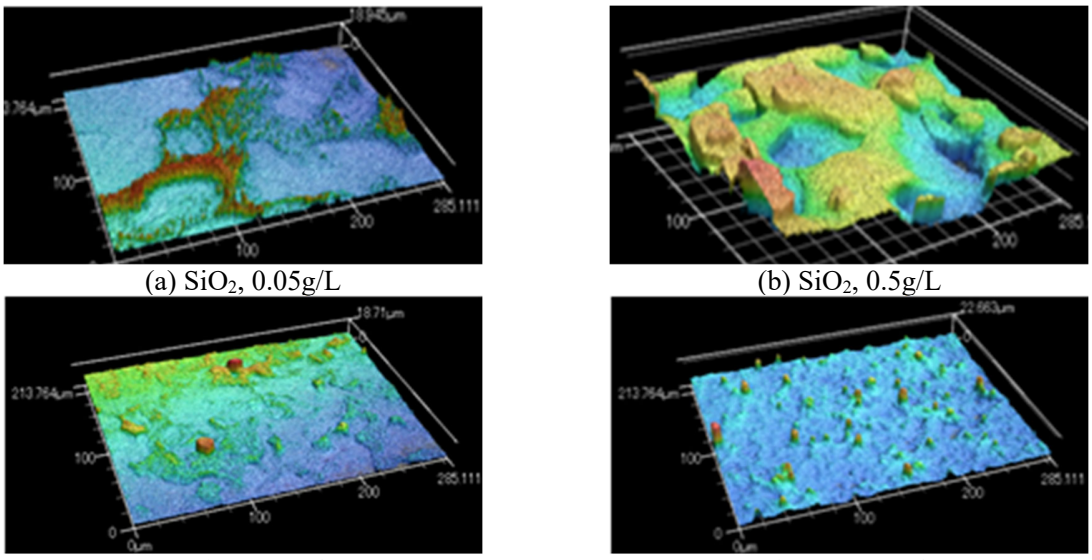

(a) SiO_2, 0.05g/L (b) SiO_2, 0.5g/L

(c) Al_2O_3, 0.5g/L (d) TiO_2, 0.5g/L

Figure 2. Images of nanoparticle layer formed on the heat transfer surface during nucleate boiling.

3. BOILING HEAT TRANSFER CHARACTERISTICS IN NANOFLUID

3.1. Experimental Results for Pure Water

As a reference data, boiling curve was measured for pure water. The result is shown with the light-blue line in Fig. 3(a). In the figure, the grey line indicates the natural convection heat transfer correlation for upward-facing surface [1], the red line the nucleate boiling heat transfer correlation by Rohsenow [18], and the black line the CHF correlation by Zuber [19]. In the low wall superheat region of $\Delta T < 10$ K, the values of heat flux q in the present experiment for pure water were higher than the natural convection correlation. In the present experiment, the stainless-steel plate was set at the tip of the copper block. This discrepancy is hence attributed to the heat loss to the stainless-steel plate. From Fig. 3(a), the heat loss is estimated less than 50 kW/m^2 and not negligible but this effect is not included in the following analyses since the main objective of this work is relative evaluation of the heat transfer performance in nanofluids. In the high wall superheat region of $\Delta T > 10$ K, the present experimental result agrees with the correlations by Rohsenow and Zuber well.

3.2. Effect of Particle Material

Figure 3(a) presents also the boiling curves for the three nanoparticle materials at the nanoparticle concentration of 0.5 g/L. Interestingly, the boiling curve was almost unchanged for TiO_2 but it shifted to the left for Al_2O_3 (improvement) while to the right for SiO_2 (deterioration). In these experiments, nanoparticle material is the sole difference between each experiment. It was therefore confirmed that the nucleate boiling heat transfer can be improved, deteriorated, or unchanged depending on the nanoparticle material. The value of CHF increased in all the nanofluids as in previous experiments reported in literature [8, 9]. The increasing rate was largest for SiO_2 and smallest for Al_2O_3. It is interesting to note that in the experiments for nanofluids, the inclination of the boiling curves tends to decrease with an increase in ΔT near the CHF condition. This tendency is particularly noticeable for SiO_2. In consequence, the value of ΔT at CHF reached 70 K.

3.3. Effect of Particle Concentration

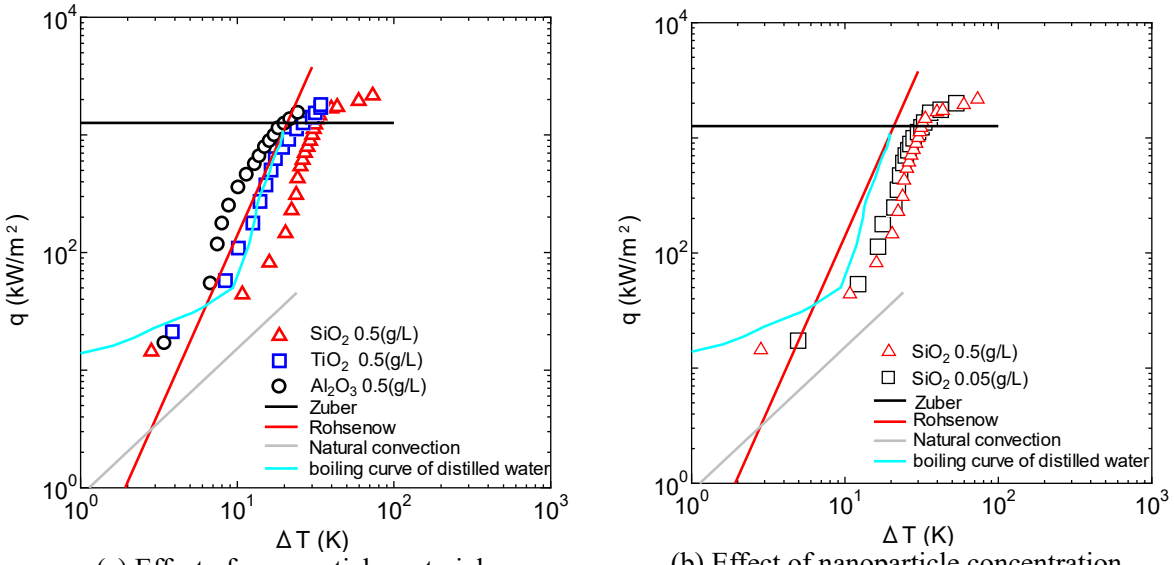

(a) Effect of nanoparticle material (b) Effect of nanoparticle concentration

Figure 3. Boiling curves for pure water and nanofluids.

To explore the effect of the nanoparticle concentration C, it was decreased to 0.05 g/L. As for the nanoparticle material, SiO_2 was selected since it showed the highest CHF value. The results are presented in Fig. 3(b). It can be seen that the reduction of C of one-tenth caused a slight improvement in HTC and slight deterioration in CHF. The dependence of HTC on C in the present experiment is similar to that for TiO_2-water nanofluid reported by Uesawa et al. [20].

4. PROPERTIES OF HEAT TRANSFER SURFACE

4.1. Effect of heat flux

Variations of the heat transfer surface properties with an increase in the heat flux are displayed in Fig. 4. It can clearly be seen that in all the four experimental conditions, the surface properties are dependent on the heat flux. Thus, variations of the surface properties with the heat flux level should be taken into consideration to understand the reason of heat transfer characteristics change in nucleate boiling of nanofluid.

4.2. Mass and Thickness

The measured mass M and thickness δ of the nanoparticle layer are presented in Figs. 4(a) and (b), respectively. Both the values tend to increase with an increase in q. Kwark et al. [21] discussed that not the gravitational force but the microlayer evaporation beneath the bubble is the main cause of nanoparticle layer formation. Since vapor bubble formation is intensified with an increase in q, the increasing trends of M and δ with an increase in q can be attributed to the increasing power to deposit the nanoparticles on the surface. In the case of TiO_2, M and δ increase with an increase in q but they decrease after the occurrence of CHF. Watanabe et al. [17] measured the adhesion strength of the nanoparticle layer and reported that it was weakest for TiO_2. It is therefore supposed that significant amount of nanoparticles was detached from the surface when the CHF condition was reached. Zuhairi Sulaiman [16] suggested that the nanoparticle layer detachment occurs not only at CHF but at lower heat fluxes. Hence, the decreasing trends of M and δ with an increase in q for SiO_2 at the concentration of 0.05 g/L can be attributed to smaller amount of nanoparticle deposition in comparison with the nanoparticle detachment at higher heat fluxes. Finally, it is interesting to note that remarkably high values of M and δ were measured at CHF and 80% CHF for the high-concentration nanofluid of SiO_2. It is expected that since the microlayer beneath the bubble is thin at high heat flux, the driving force to deposit the nanoparticles on the surface is intensified near CHF. In addition, the SiO_2 nanoparticles adhere the surface tightly [17]. In consequence, the deposition surpassed by far the detachment to increase M and δ significantly in this case.

4.3. Roughness

Comparison of Fig. 4(c) with Figs. 4(a) and (b) indicates that the surface roughness Ra increases with M and δ. Okawa et al. [15] found that the nanoparticle layer deposition occurred mainly at the active nucleation sites. This observation is consistent with Kwark et al.'s theory [21]. It is therefore understandable that the nanoparticle layer is not formed uniformly on the surface and consequently Ra should increase in rough proportion to M and δ. This indicates the possibility that the nanoparticle layer surface has the asperity of the wavelength associated with distance between the active nucleation sites. The change in the surface roughness is often regarded as one of the main reasons to cause HTC modification in nanofluid nucleate boiling [8]. It is however probable that the surface morphology of the nanoparticle layer has two characteristic length scales associated with the original roughness of shorter length scale and the distance between the active nucleation sites of longer length scale. Investigating the contribution of roughness of each length scale might be of importance in the future study.

4.4. Wickability

The measurement results of wickability *Wi* are presented in Fig. 4(d). As in the other factors, *Wi* tends to increase with an increase in *q*. The nanoparticle layer plays a role as a passive pump to suck liquid using capillarity of porous structure. *Wi* may be regarded as the factor to associated with the pump quantity. It is hence expected that *Wi* increases with δ. This expectation is generally true but the relation is not always linear. For instance, the value of δ for SiO_2 of 0.5 g/L increases significantly at CHF and 80% CHF in Fig. 4(b), the variation of *Wi* is not remarkable in Fig. 4(d). Since the nanoparticle layer develops rapidly, many defects might be created inside it to prevent linear increase of *Wi* under high-heat-flux conditions.

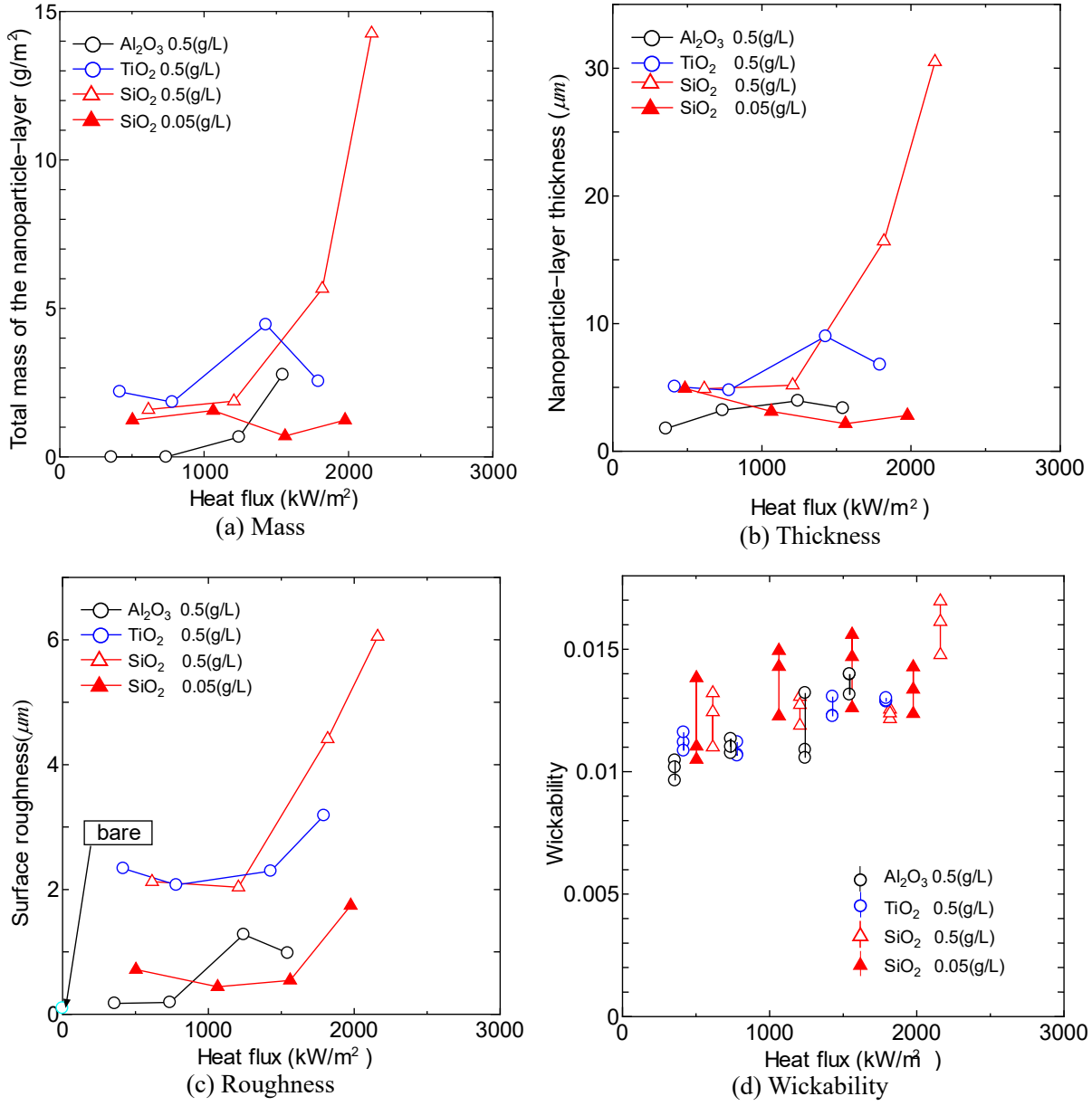

Figure 4. Properties of nanoparticle layer formed on the heat transfer surface.

5. DISCUSSION ON MECHANISMS OF BOILING HEAT TRANSFER MODIFICATION

5.1. CHF

To explore the reason of CHF enhancement in nanofluids, the values of CHF are plotted against *Wi* following Rahman et al. [14]. It can be seen that CHF tends to increase with an increase in *Wi* as reported by Rahman et al. for structured superhydrophilic surfaces, but the CHF value for Al_2O_3 is noticeably lower than those for other nanofluids. It may be attributed to the surface roughness, since the value of *Ra* was noticeably smaller for Al_2O_3 as shown in Fig. 4(c).

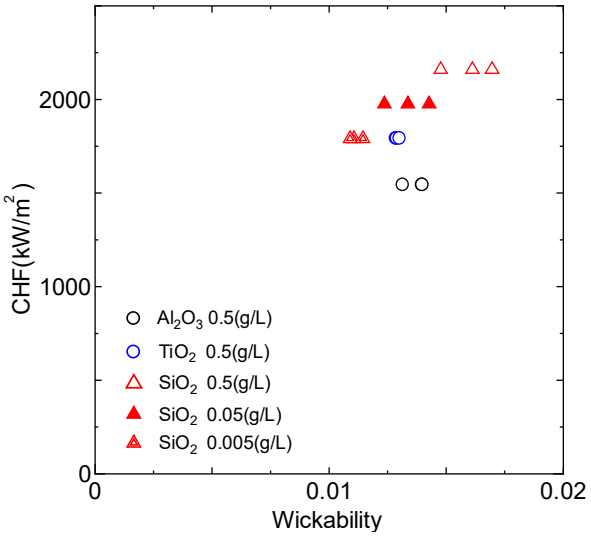

Figure 5. Dependence of CHF on *Wi*.

5.2. HTC

The relation between HTC and δ is presented in Fig. 6(a). Here, HTC values were scaled using Rohsenow's correlation. It can clearly be seen that HTC decreases with an increase in δ. This would be the evidence the deterioration of nucleate boiling heat transfer is caused mainly by the surface effect that is the thermal insulation by the nanoparticle layer. However, the thermal insulation effect can never be the reason of the HTC enhancement. To explore the reason of HTC enhancement, the working liquid was replaced by pure water after the CHF experiment for the Al_2O_3 nanofluid. The obtained boiling curve is displayed in Fig. 6(b). Surprisingly, the HTC enhancement disappears completely and the boiling curve shifted to the right. This indicates that the HTC improvement observed in this experiment was caused mainly by the bulk fluid effect. Since the thermal conductivity often increases noticeably in nanofluid, this would be most probable as the main cause of the HTC enhancement.

It should be noted that the heat transfer coefficient in the present work is defined by the temperature difference between the surface temperature of the copper block and the saturation temperature of boiling fluid. Thus, the measured boiling heat transfer coefficient is in some sense the overall heat transfer coefficient containing the boiling heat transfer resistance on the nano deposited particle layer surface and the thermal conduction resistance in the layer; not the boiling heat transfer coefficient of the nano layer surface. Further examination is required.

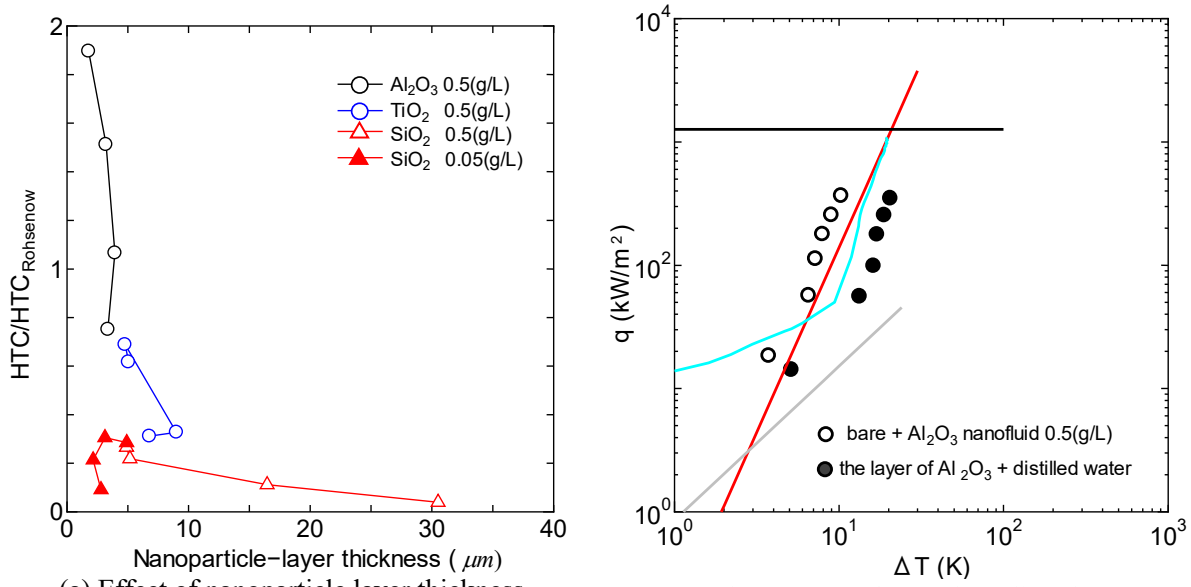

(a) Effect of nanoparticle layer thickness (b) Effect of the working liquid

Figure 6. Dependences of HTC on δ and working liquid.

6. CONCLUSIONS

Distilled water-based nanofluid pool boiling experiments at 0.1 MPa were performed using TiO_2, Al_2O_3 and SiO_2 as the nanoparticle materials to explore the mechanisms to cause the changes of the HTC and the CHF values in the nanofluid nucleate boiling. In the experiments, the thickness, the surface roughness, the wickability, and the total mass of the nanoparticle layer formed on the heat transfer surface were measured. Main conclusions of this work are summarized as follows.

(1) Although CHF was enhanced for all the nanoparticle materials, HTC was not changed in the case of TiO_2, augmented in the case of Al_2O_3 and deteriorated in the case of SiO_2. Generally, the thickness, the total mass and the surface roughness of the nanoparticle layer increased with an increase in the heat flux since the nanoparticles are deposited on the heat transfer surface beneath the bubble produced during nucleate boiling. The wickability was also increased with an increase in the heat flux.
(2) It was discussed that CHF increased mainly with an increase in the wickability but surface roughness also contributed to the CHF enhancement.
(3) HTC is determined by the competition between deterioration caused by the surface effect (thermal-insulation effect of the nanoparticle layer) and improvement caused by the bulk fluid effect (change in the liquid thermal conductivity).

ACKNOWLEDGMENTS

This work was supported by MEXT Innovative Nuclear Research and Development Program Grant Number JPMXDO219213883.

REFERENCES

1. F.P. Incropera, D.P. DeWitt, A. Lavine, T.L. Bergman, *Fundamentals of Heat and Mass Transfer, 6th ed.,* Willey, New York, (2006).

2. P.B. Whalley, *Boiling, Condensation, and Gas-Liquid Flow*, Chaps. 16 and 17, Clarendon Press, Oxford, UK (1987).
3. V.P. Carey, *Liquid-Vapor Phase Change Phenomena, 3rd ed.*, Chap. 12, CRC Press, Boca Raton, FL, USA (2020).
4. J.G. Collier, J.R. Thome, *Convective Boiling and Condensation, 3rd ed.*, Chap. 6, Clarendon Press, Oxford, UK (1994).
5. J.M. Wu, J. Zhao, "A review of nanofluid heat transfer and critical heat flux enhancement - Research gap to engineering application," *Progress in Nuclear Energy*, **66**, pp. 13-24 (2013).
6. R. Kamatchi, S. Venkatachalapathy, "Parametric study of pool boiling heat transfer with nanofluids for the enhancement of critical heat flux: A review," *International Journal of Thermal Sciences*, **87**, pp. 228-240 (2015).
7. L. Cheng, E.P. Bandarra Filho, J.R. Thome, "Nanofluid two-phase flow and thermal physics: A new research frontier of nanotechnology and its challenges," *Journal of Nanoscience and Nanotechnology,* **8**(7), pp. 3315-3332 (2008).
8. D. Ciloglu, A. Bolukbasi, "A comprehensive review on pool boiling of nanofluids," *Applied Thermal Engineering,* **84**, pp. 45-63 (2015).
9. M.S. Kamel, F. Lezsovits, "Boiling heat transfer of nanofluids a review of recent studies," *Thermal Science,* **23**(1), pp. 109-124 (2019).
10. S.M.S. Murshed, K.C. Leong, C. Yang, "Thermophysical and electrokinetic properties of nanofluids - A critical review," *Applied Thermal Engineering,* **28**(17-18), pp. 2109-2125 (2008).
11. S.M. Kwark, R. Kumar, G. Moreno, J. Yoo, S.M. You, "Pool boiling characteristics of low concentration nanofluids," *Int. J. Heat. Mass Transf.,* **53**, 972-981 (2010).
12. Z. Shahmoradi, N. Etesami, M.N. Esfahany, "Pool boiling characteristics of nanofluid on flat plate based on heater surface analysis," *Int. Commun. Heat. Mass Transf.,* **47**, 113-120 (2013).
13. R.V. Pinto, F.A.S. Fiorelli, "Review of the mechanisms responsible for heat transfer enhancement using nanofluids," *Applied Thermal Engineering,* **108**, pp. 720-739 (2016).
14. M.M. Rahman, E. Ölçeroglu, M. McCarthy, "Role of wickability on the critical heat flux of structured superhydrophilic surfaces," *Langmuir*, **30**(37), pp. 11225-11234 (2014).
15. T. Okawa, M. Takamura, T. Kamiya, "Boiling time effect on CHF enhancement in pool boiling of nanofluids," *International Journal of Heat and Mass Transfer,* **55**(9-10), pp. 2719-2725 (2012).
16. M. Zuhairi Sulaiman, D. Matsuo, K. Enoki, T. Okawa, "Systematic measurements of heat transfer characteristics in saturated pool boiling of water-based nanofluids," *International Journal of Heat and Mass Transfer,* **102**, pp. 264-276 (2016).
17. Y. Watanabe, K. Enoki, T. Okawa, "Nanoparticle layer detachment and its influence on the heat transfer characteristics in saturated pool boiling of nanofluids," *International Journal of Heat and Mass Transfer,* **125**, pp. 171-178 (2018).
18. W.M. Rohsenow, "A method of correlating heat-transfer data for surface boiling liquid," *Trans ASME*, **74**, pp.969-976 (1952).
19. N. Zuber, "The hydrodynamic crisis in pool boiling of saturated and subcooled liquids," *International Heat Transfer Conference* **27**, pp. 230-236 (1961).
20. S. Uesawa, Y. Koizumi, M. Shibata, H. Yoshida, "Study on pool nucleate boiling heat transfer of suspension liquid with deposits on heat transfer surface," *Thermal Science and Engineering,* **25**(2), pp. 17-26 (2017).
21. S.M. Kwark, R. Kumar, G. Moreno, J. Yoo, S.M. You, "Pool boiling characteristics of low concentration nanofluids," *Int. J. Heat. Mass Transf.* **53**, 972-981 (2010).